Yuhua ZOU[1], **Weihai CHEN**[1], **Dehan LUO**[2]

School of Automation Science and Electrical Engineering, Beihang University (1), School of Information Engineering, Guangdong University of Technology (2)

Virtual Physics Framework for Multi-Robot Chemical Plume Tracing under Ventilated Indoor Condition

Abstract. *This paper presents a virtual-physics based control framework for swarm robotic chemical plume tracing and source localization problem under ventilated indoor environment with complex turbulent conditions. The control force includes three kinds of effort, which are lattice formation force, plume tracing force, and obstacle avoidance force. The plume tracing and source identify strategy are based on the chemical mass flux passing through the robot colony. Simulation results show that the proposed control framework and tracing strategy can effectively navigate the multi-robot system to the chemical source emitter region. The virtual-physics based framework is highly flexible, endows the robot formation the properties of self-organization and self-repair. Compare to traditional approaches, the mass flux driven plume tracing can inhibit the robots from adhering to the obstacle-induced local density maxima and guide the robots forward to the real source region.*

Streszczenie. *W artykule opisano metodę śledzenia smugi dymu chemicznego przy wykorzystaniu robotów oraz metodę wykrywania źródła dymu w pomieszczeniu wentylowanym przy zawirowaniu powietrza. Stosowane są trzy środki – określenie siatki, śledzenie dymu i eliminacja zjawiska. Roboty śledzące mogą się same organizować i naprawiać. W porównaniu do innych metod zaproponowana metoda zabezpiecza roboty przed zatrzymaniem się przy lokalnym maksimum i prowadzi je do źródła dymu.* ***(Wykorzystanie multi-robotów do śledzenia dymu w wentylowanych pomieszczeniach)***

Keywords: chemical plume tracing, sensor networks, swarm robotics, virtual-physics
Słowa kluczowe: smugi chemiczne śledzenia, sieci czujników, rój robotów, virtual-fizyka

Introduction

In recent years the number of studies on application of robotic odor-sensing technology has increased substantially. Mobile robots equipped with chemical sensors can be useful for a number of application areas, for instance, to monitor poisoned areas for leaks, to find hidden explosives, to search for survivors following a disaster, and to detect leaks in industrial environments. Instead of humans, robots can be dispatched to areas with odor contamination for inspection, or providing continuous monitoring of the contaminated environment for specific characterization of the odor. Such tasks are named as Chemical Plume Tracing (CPT) or Odor Source Localization. Employing multiple robots can further improve performance since they can do the search cooperatively in parallel. To achieve these goals there is a need for developing efficient algorithms for coordination between robots as well as robotic search, exploration, and coverage. One possibility is to use the virtual physics (VP) framework, which is efficient, scalable, robust, and subject to rigorous theoretical analysis and predictions [1].

In this paper, we propose a CPT algorithm using the lattice formations, built with virtual physics force (VPF), as a distributed sensor and computation network that acts as a parallel computer for performing fluid flow analysis to assist in the making of navigational decisions. In addition, the paper also focuses on an evaluation of three plume-tracing algorithms on a suite of realistic flow simulations, including a challenging set of obstacle courses, and shows that the use of fluid mechanics improves swarm performance on the CPT task.

Problem Definition

Consider an application in which a group of robots are required to perform a search in an unknown environment contaminated with a chemical substance. The chemical substance is possibly dangerous for human beings. Therefore, search by autonomous robots is more suitable to the problem. Moreover, employing multiple robots in parallel search may possibly lead to a faster and more effective performance. Assume that the robots are equipped with the necessary hardware and are able to sense the chemical (or set of chemicals) which contaminate the environment. The objective is to build the map of chemical concentration as well as to determine the region with the highest concentration of the contaminant. Such information might be useful for experts who may determine whether the concentration level of the chemical is within tolerable levels or constitute a danger. If there are more than one chemicals contaminating the environment and the robots are equipped with chemical sensor arrays and can sense and distinguish different chemicals, it might be possible to determine the composition of the chemicals contaminating the environment. This, on the other hand, can provide extra useful information about the sources and severity of contamination. Higher chemical concentration areas usually occur very close to the sources of chemicals and determining the regions with high concentration might give information of the positions of the leaks (i.e., chemical sources) contaminating the environment. Such a situation can arise in, for example, a building (such as a large warehouse) under fire where burning of certain chemicals might be really dangerous since certain levels of some chemicals might lead to explosion. Moreover, the composition of the chemicals might give an idea of what are the burning materials. All this information can be collected by the robots without endangering the lives of firefighters and critical decisions might be taken (e.g., a decision such as whether to go into the building or not) based on the information obtained by the robots. Other applications can include disaster situations in chemical or nuclear plants (provided that the robots are equipped with the necessary sensing hardware) and security or defense applications.

In order to be able to perform efficient search, the robots should be able to pass their sensor readings as well as other needed information among each other. Moreover, they are required to pass the information they have gathered to a remote computer (a base station) where the data should be collected and combined. The task is to search an unknown environment with multiple-robots with the objective to locate the highest concentration of the gas.

Related Work

The mobile robots CPT problem is essentially a search problem in chemical space. The purpose of this problem is to search and finally determine the location of the chemical source. Several research groups have been working on this area since earlier of 1990s. Typical strategies and meth-

ods designed for plume tracing and source localization include imitation of animal behavior [2, 3], logical determination [4], plume tracing [5, 6, 7, 8], artificial neural network [9], probability estimation [10] and multiple robots cooperation [11, 12, 13, 14]. Since a CPT system must measure concentration of the trace chemical, the most widely utilized approach is $gradient$ strategy, which follows a local gradient of the chemical concentration within a plume [15, 16, 17]. Another popular biomimetic approach is $upwind$ strategy. An wind-driven agent observes the direction of fluid flow, and navigates upstream inside the plume [11, 18]. Wandel [19] performed laboratory plume mapping experiments with a single mobile robot, and found that the chemical density profiles are spatially stable over significant lengths of time. Russell and Purnamadjaja [20] developed an odor recognition system consisting of an array of chemical and airflow sensors capable of identifying the type of a trace chemical, and estimating the direction of the source. Both of these systems used a small suction fan to move the air past the stationary chemical sensors, similar in principle to the odor compass developed by Ishida, et al. [21].

The experiments in most of the CPT studies have been carried out with a single odor source and/or a single robot through a predetermined navigation algorithm to explore the environment and to search for the source [22, 23]. In [24] odor classification and gas distribution are combined for source localization and gas distribution map building. There multiple odor sources are used and the resulting gas distribution map is combined with the laser range finder and sensor data of a single robot. In other related studies chemical gas concentration map of the unknown environment is obtained by means of Gaussian weighted functions and concentration grid maps methods [25]. Furthermore, swarming algorithms [11] and predefined path tracking algorithms [26] are used to localize odor sources. A. T. Hayes et al. [11] presented an investigation of odor localization by groups of autonomous mobile robots using principles of Swarm Intelligence (SI), a computational and behavioral metaphor for solving distributed problems that takes its inspiration from biological examples provided by social insects. R. A. Russell [27] has developed an odor marking and detection system for mobile robots. Such a system will provide the basis for investigating the use of odor markings as an aid to mobile robot navigation. Zarzhitsky et al. [28] propose a cooperative group of robots moving in a close formation, also using fluid-dynamics information. Most of these approaches are suitable for applications in static environments. However, these algorithms have not been tested in an environment with multiple real contaminating sources. Such an environment is expected to be less ideal (more dynamic) and bring new challenges in addition to the practical/experimental difficulties.

Common methods for managing distributed autonomous systems, and robotic swarms in particular, include those that use ad-hoc and loosely connected structures, model specific behaviors, follow a set of rules, or employ control-theoretic methods based on optimization of system equations [11, 29, 30]. Over the course of the last decade, a physics-inspired methodology has emerged as a successful alternative for achieving complex aggregate behavior from a group of simple robots, e.g., [31, 32]. This is the approach embodied by the virtual physics framework. The term “virtual" (sometimes referred as artificial) is used because this framework is motivated by natural physical forces and robots act as if they are real. Yet we are not restricted to emulation of commonplace physics, and have the freedom to develop our own force laws to achieve our objective. VP is a distributed control framework for applying virtual physics forces to construct multi-robot formations with flexible configuration. Potential energy is minimized, but without the expense of global potential fields calculations [33]. Unlike explicit kinetic energy formulations [34], VP uses inter-agent forces directly. Even though VP does not attempt to match the optimality offered by control-theoretic approaches [35, 30], its performance is excellent [1].

Relationship Between Chemical Mass Flux and Source Identify

The proposed CPT method basically relies on the chemical mass flux passing through the robot lattice, so this section provides a short review of the relevant material. Fluid flow is governed by three fundamental laws: conservation of mass, conservation of momentum, and conservation of energy. The law of mass conservation can be expressed as:

$$\frac{\partial \rho}{\partial t} = \nabla \cdot (\rho V) \tag{1}$$

where ρ is the mass density of the chemical, V is the fluid's velocity, and t denotes time. The product ρV is called the mass flux, which represents the time rate of change of mass flow per unit area. The RHS of ((1)) is called the mass flux divergence (MFD), and in 2D Cartesian coordinates is given by:

$$\nabla \cdot (\rho V) = u\frac{\partial \rho}{\partial x} + \rho\frac{\partial u}{\partial x} + v\frac{\partial \rho}{\partial y} + \rho\frac{\partial v}{\partial y} \tag{2}$$

where $V = u\vec{i} + v\vec{j}$. $\vec{i}$ and $\vec{j}$ are unit vectors in the x and y coordinate directions, respectively. For a spatial point P, if $\nabla \cdot (\rho V) > 0$, then it means that point P is a source emitter, while $\nabla \cdot (\rho V) < 0$ indicates a sink (potentially a plume “trap” that consists of high local chemical concentration). According to the Divergence Theorem of vector calculus:

$$\int_W \nabla \cdot (\rho V)\, \mathrm{d}W = \oint_S (\rho V)\, \mathrm{d}S \tag{3}$$

where W is the control volume and S is the bounding surface of the volume, if the robots surround a suspected emitter, and the total mass flux measured by the sensor grid consistently exceeds some small, empirically-determined threshold, then the robots have localized the emitter [28]. This result serves as the important criterion for theoretically identifying a chemical emitter. In addition, we also apply the mass flux information to drive a mobile swarm via local plume observations, which is described in next section.

The Virtual-Physics based Control Framework

To solve the plume tracing problem, we proposed a virtual physics-based framework to control the robots by imitating the forces that exist within real-world particle systems. Although these forces are defined only inside the control software, the robots act as though the forces are real. Such control methodology is simple - there is no need for a global controller, or long-range communication [36]. Instead, each individual observes the environment, notes the position of nearby robots, and then computes a control force vector that alters its route. The control method enforces Newton's Laws, such as $conservation\ of\ momentum$ and the basic $F = ma$ equations. Generally, the control force includes three kinds of effort, which are lattice formation force, plume tracing force, and obstacle avoidance force.

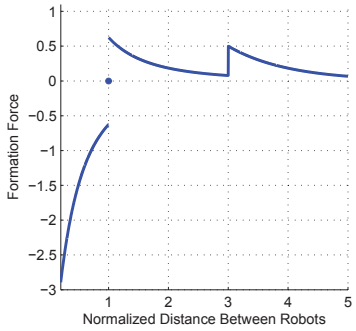

Fig. 1. The lattice formation force law with parameters, $G = 5$, $p = 3$, $\delta = 0.5$

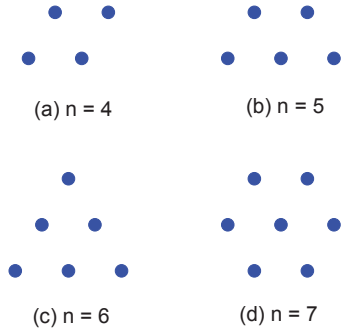

Fig. 2. Four usual formations with different robot number n

Lattice Formation Force

Using a simple geometric construction, the robots only need to know the range and bearing to their neighbors in order to form a certain size lattice structure [32]. In our study, we define the lattice formation force as a function of the distance between neighboring robots as follows:

$$F_f = \begin{cases} -G/(d+1)^p & if\ d < 1 \\ 0 & if\ d = 1 \\ G/(d+1)^p & if\ 1 < d < 3 \\ \delta \cdot e^{3-d} & if\ d \geq 3 \end{cases} \tag{4}$$

where $d = r/D$ represents the normalized distance between nearby units, with parameter r denotes the actual distance between the robots and D is the desired separation; G is a universal constant and p is a power value that determine the magnitude and slope of the formation force. Neighbor robots repel each other when F_f is negative, and attract when F_f is positive. When $r > D$, the magnitude of the formation force decrease with the increasing distance between nearby units. In case of the robot lag behind during the plume tracing stage, we set a step-like jump in magnitude at $r = 3D$ with a parameter δ range from 0 to 1 (see Fig. 1).

The force law is inverse-power law of distances incorporating both attraction and repulsion, similar to those found in molecular dynamics. Attraction dominates over long distances and repulsion dominates over short distances. Using this force law, the resulting system displays 'social' behaviors such as clustering, guarding, and escorting. Four usual formations corresponding to different robot numbers on the basis of the above formation force law are illustrated in Fig. 2. The distance value between two nearby robots is stable at D, and the separation angle is stable at $60°$. Most commonly, seven agents would arrange in a hexagonal formation. Since hexagonal tiles can tile a planar region (i.e., the hexagonal grids can be connected without spatial gaps), this geometry is particularly well suited for sensor applications [37].

The reactive nature of the formation law ((4)) allows for straightforward recovery from unexpected events, such as loss of sensor nodes or operation in unstructured environments [1], and endows the system with valuable properties, such as self-organization and self-repair [32].

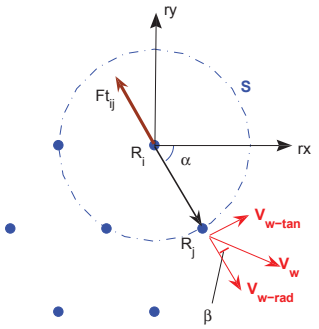

Fig. 3. Sketch map of the plume tracing force

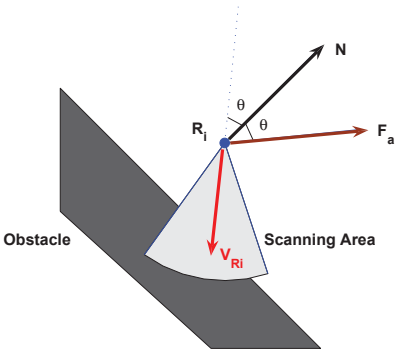

Fig. 4. Sketch map of the obstacle avoidance behavior

Plume Tracing Force

In order to accomplish tasks other than organizing the swarm into a formation, the virtual physics-based framework should incorporate mission-specific goal forces. For the CPT problem, we introduce a plume-tracing force as the goal-directed force. The plume tracing strategy is actually mass-flux-driven. When the robots are mapping a chemical plume, they periodically share their sensor observations (including odor concentration or chemical mass density, wind speed and wind direction) with the neighboring partners, and use these data to calculate the plume-tracing force which allows them to the odor source emitter.

Figure 3 shows how each robot computes the chemical mass flux (CMF) and the plume tracing force. S is a closed circle with radial D and centers on the position point of robot R_i. The robots on and in the circle S are considered as the neighbors of robot R_i. Suppose that robot R_j is one of the neighbors of robot R_i. At time t, the azimuth angle of R_j to R_i is α. The chemical mass density and the wind velocity at the position of R_j is $\rho(j,t)$ and $V_w(j,t)$, respectively. The included angle of azimuth α and wind direction is β. Then the radial CMF passing through robot R_j at time t is given by:

$$M_{rad}(j,t) = \rho(j,t) \cdot V_w(j,t) \cdot \cos(\beta) \tag{5}$$

We define the CMF passing through the bounding surface S as a sum of the radial CMF flowing through the neighboring partners of robot R_i, so the RHS of ((3)) is calculated in a simplified expression:

$$\oint_S (\rho V) \cdot dS \approx \sum_{j \in Neighbor(\mathrm{R}_i)} M_{rad}(j,t) \tag{6}$$

There is an acting force between robot R_i and robot R_j

as a function of the azimuth angle α and the radial CMF $M_{rad}(j,t)$:

$$F_t(i,j,t) = -K_t \cdot M_{rad}(j,t) \cdot \cos(\alpha) \tag{7}$$

where K_t is a constant that determines the magnitude of the acting force. And the plume tracing force for robot R_i is a composite force from all the acting force between R_i and its neighbors:

$$F_t(i,t) = \sum_{j \in Neighbor(\mathrm{R}_i)} F_t(i,j,t) \tag{8}$$

If the radial CMF of R_j is positive, i.e. $M_{rad}(j,t) > 0$, it means that the chemical fluid at the location of R_j is flowing out of the control volume, and R_j is on the leeward side, so robot R_i will be pulled away from R_j; otherwise, robot R_i will be pushed toward R_j. This force takes effect in such way that, robot R_i can always move opposite to the fluid direction until it arrive at the source emitter area, and prevents itself from getting bogged down in a plume "trap" .

Obstacle Avoidance Force

While the robots move toward the source emitter, they may confront several obstacles or walls impeding their tracing route. To avoid collision, each robot scans its front area with a certain scanning angle and radius (see Fig. 4). Once an obstacle is detected in the scanning area, the robot implement avoidance behavior similar to the mirror reflection law: suppose the normal of the estimated collision face of the obstacle is N, the corresponding normal direction is γ_N, the velocity of robot R_i at time t is $V_R(i,t)$, and the incidence angle, i.e. the include angle θ between N and $V_R(i,t)$ is:

$$\theta = \pi - \operatorname{acos}\left(\frac{(N, V_R)}{|N| \cdot |V_R|}\right) \tag{9}$$

Considering the positions of the obstacle and robot R_i, the direction $e(i,t)$ of the obstacle avoidance force $F_a(i,t)$ is expressed as follows:

(10)
$$\begin{cases} e(i,t) = \gamma_N - \theta & \text{obstacle on right hand side of } \mathrm{R_i} \\ e(i,t) = \gamma_N + \theta & \text{obstacle on left hand side of } \mathrm{R_i} \end{cases}$$

The magnitude of the avoidance force is specified constant K_a.

By balancing the internal formation forces and the external plume tracing / obstacle avoidance forces, we can show that the group of robots can maintain its grid-like sensor arrangement while also moving toward the chemical source emitter location (see Fig. 5).

Chemical Plume Tracing Strategy

The proposed chemical plume tracing strategy consists of three stages: swarm together into a stable formation, find the chemical plume and trace it, finally locate and verify the source emitter.

Swarming Stage

At the beginning, all the robots are distributed randomly in a limited entrance area. Then the robots start swarming together driven by the inner cohesive force. Until the robots construct a stable lattice grid, they do not process any environmental information from the chemical sensor.

Plume Finding and Tracing Stage

Traditionally, there are two common approaches to find and trace the chemical plume, which are gradient strategy and upwind strategy. The gradient strategy simply follows the chemical gradient, so the direction of the largest chemical concentration is the goal direction. However, such approach will easily cause the robots to find pockets of high local chemical concentration, as opposed to finding the true chemical emitter. The upwind strategy always moves upwind while inside the chemical plume. But obviously, the changeable instantaneous fluid velocity is not a reliable indicator of an emitter's location. The instantaneous wind direction does not always point to the chemical emitter, but rather to the current wind source.

In our study, we introduce a mass-flux-driven strategy which combines information about both fluid velocity and chemical density to improve the plume tracing performance of the formation. After the robots finish clustering, they start to receive and share the sensor observations (including odor concentration or chemical mass density, wind speed and wind direction) with each other. If the wind speed or the chemical mass density is too low to form a strong enough plume tracing force, the robots will execute traditional casting method. It typically consists of a zigzag or spiraling motion to increase exploration [10, 11].

Once the chemical plume is detected, the robots shares flow-field variables with their neighbors, and use these values to calculate the next waypoint. Each robot maps the shared sensor data to its own coordinate axes, independently calculates the best direction to search next, and then translates it into a virtual goal force. The final driving force for each robot consists of a vector sum of the lattice formation force, plume tracing force and obstacle avoidance force vectors. The resulting effect is that the entire group moves in formation toward the chemical source.

Source Emitter Verification Stage

When arriving at the emitter region, because of the balance of the inner formation force and external plume tracing force, the robots get bogged down and become a ring surrounding the potential source emitter. According to ((2)), we can verify a region with positive mass flux divergence by measuring the total flux exiting the region. This can be easily calculated via using (6).

Simulation Experiments

The simulation studies detailed in this paper was divided into two major categories. First, we evaluate a set of simulated scenarios designed to model the ventilated indoor environment with a small swarm of robots, and then we increase the number of agents in simulation to verify the scalability and robustness of our method. Three kinds of CPT algorithms, i.e. gradient-driven, wind-driven and flux-driven, are simulated and compared.

In the first set of experiments, a hexagonal lattice of seven robots was used, coupled with an performance metric, namely, the $enclosure\ frequency$ of the source emitter by the lattice. In the second set of experiments, a swarm of robots with increasing size was used. As our main concern here is the effects of the swarm size on CPT performance, the previous enclosure metric is no longer adequate. Instead, we recorded the total number of emitter detections by the robotic swarm, called the $localization\ frequency$. Besides, we also uses an additional performance metric, namely, the amount of time it takes to locate the emitter, called the $arrival\ time$ by any robot. This second metric illuminates the relationship between swarm size and CPT speed.

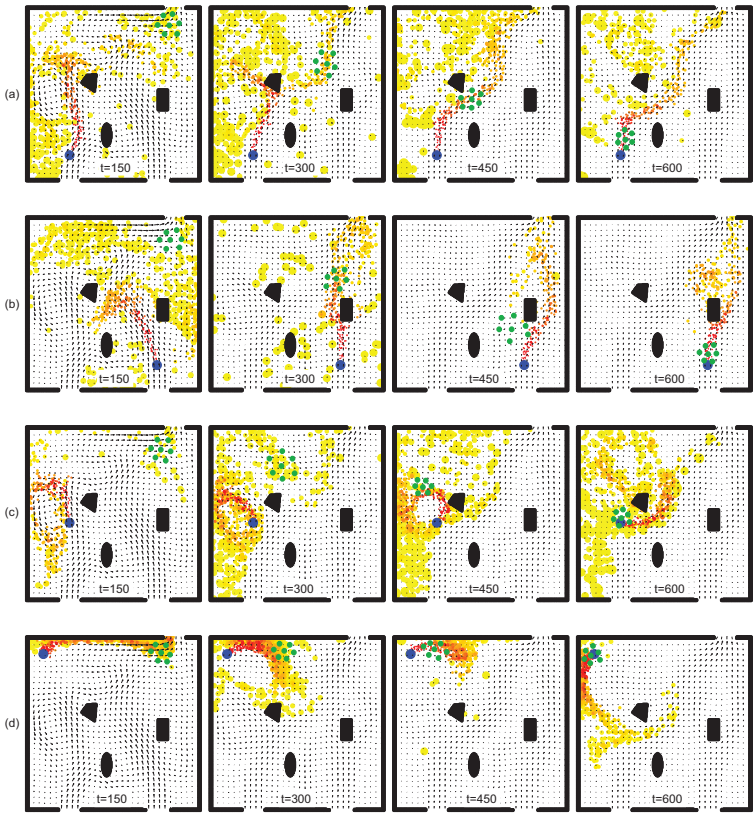

Fig. 5. Four simulated flux-driven plume tracing sequences: heavier chemical concentration is shown with varying colors from yellow to red; the collection of green circles is the robotic swarm, which starts out in the top right corner, and successfully finds the emitters, denoted by blue circles. Arrows depict wind velocity.

Experimental Model of the Plume

All of the reported simulation results rely on a plume model by Farrell et al. [10], chosen because of its efficiency, realism (i.e., its instantaneous and time-averaged results match measurements of actual plumes), and multi-scale properties - including chemical diffusion and advective transportation. Different from other continuous, time-averaged models, the chemical plume we used is discrete, consisting of a collection of localized “puffs" of the trace element. Note that the model does not include boundary conditions (it is more suitable for outdoor conditions with no boundaries). So we extended the original equations to incorporate obstacles. The flow field of large-scale eddy is calculated by FLUENT software, so that it enhances the authenticity and accuracy of the flow field. This extended model is mainly used in the simulation of odor plume under ventilated indoor condition.

The simulation environment is a 10m$\times$10m ventilated lab. The outside flow enters the lab from two windows on the bottom wall, and exits from a door at top right corner. Figure 5 illustrates four typical distribution sequences of plumes released at four different locations in a limited indoor area. The odor sources in Fig. 5(a) and Fig. 5(b) are near the left and right window, respectively. In Fig. 5(c) and Fig. 5(d), the odor sources are near the left middle area and upper left corner, respectively. It can be found that the puffs has local maximum when the emitter is near corners. Due to the complex turbulent flow conditions, the chemical plumes are highly time varying in direction.

Experimental Model of the Odor Sensor

Metal Oxide Semiconductor (MOS) sensors are widely used in the practical experiments of odor source localization. The simulation experiments here also adopt the model based on MOS sensors. Unlike other types of rapid-response sensor, most MOS sensors have a considerable reaction time with chemicals, which is an important factor on the CPT performance. So without loss of generality, we only model the response and recovery time of the MOS sensor (see Fig. 6). The nonlinear relationship between the input concentration and the output resistance value is not considered.

The response and recovery stages of MOS sensors are both regarded as second-order inertia link approximately. As shown in Fig. 6, we adopt a phase switch module to select the sensor’s reaction phases based on the information from the input signal and the feedback of the output signal. When the output feedback is bigger than the input, the recovery phase is chosen; Otherwise, the response phase is chosen. The decentralized sensor model with Gauss noise are expressed as follows.

- Response phase

$$(11)\quad \begin{cases} y_{res}(k) = a_{res}x_{res}(k) + b_{res}y_{res}(k-1) \\ \qquad\qquad + c_{res}y_{res}(k-2) + n_{res}(k) \\ a_{res} + b_{res} + c_{res} = 1 \end{cases}$$

- Recovery phase

$$(12)\quad \begin{cases} y_{rec}(k) = a_{rec}x_{rec}(k) + b_{rec}y_{rec}(k-1) \\ \qquad\qquad + c_{rec}y_{rec}(k-2) + n_{rec}(k) \\ a_{rec} + b_{rec} + c_{rec} = 1 \end{cases}$$

Referring to the estimation of the sensor response of Figora’s TGS gas sensors in [38], the design parameters for the two phases are set differently so that the response time is about 2 seconds and the recovery time is about 10 seconds (see Fig. 7).

Experimental Models of the Robots

To simplify simulation, some assumptions are made. The robots are assumed as particles. Each robot is equipped with one MOS gas sensor and one wind direction sensor, and can determine its position and orientation with odometer and an overhead camera.

Considering the influence of the recovery and response time of the MOS sensors, the robots would move in a so called 'run-stop-run-stop' mode, with the maximum speed of 0.5 m/sec. Each robot stops at one position for 10 seconds to collect the environmental information. Then the robot runs for 1s again according to the velocity and direction calculated by the algorithm. The sampling rate is set to be 0.1s. The sensor and communication range of simulated agents is limited to 1 m. The robots start to search after the odor source has leaked for 100 seconds. The total time of a complete CPT evaluation run is set to 900s. The starting locations of the robots are closed to one side of the door. Figure 5 also presents four series of snapshots of the search process with seven robots in the plume environment with different odor source locations.

In the first set of experiments, all of the plume tracing algorithms employ a hexagonal lattice of seven robots, with one in the center of the formation. To compensate for the small number of vehicles, the CPT algorithms can expand and contract the radius of the formation to improve the spatial resolution of plume sensors. This swarm behavior is accomplished within the VP framework via a local change of the neighbor separation D in ((4)) for each vehicle. Given the small size of the swarm, the VP parameters are configured to produce a strong cohesive formation force, so that a solid-like lattice formation is preserved during navigation around obstacles.

The second experimental set is oriented toward the investigation of the scalability characteristics of the VP framework. We still use the same vehicle model as before, but increase the swarm size. This change also requires certain modification on the CPT algorithms, as the larger swarm size implies the need for more flexible formations in order to pass through narrow passages and satisfy other environmental constraints. The navigation planning routines execute independently on each vehicle, resulting in a completely distributed control, fluid-like swarm motion, and increased effectiveness in negotiating around complex multi-obstacle environments. These experiments demonstrate that the self-organization and autonomous recovery capabilities of the VP framework can effectively improve the swarm performance on the CPT task.

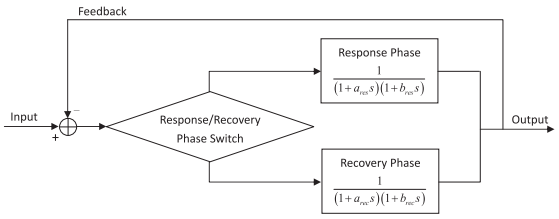

Fig. 6. The transfer function of the sensor model

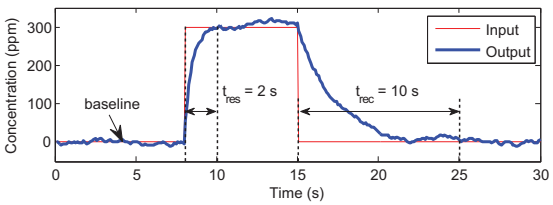

Fig. 7. The input and output sample of the sensor model

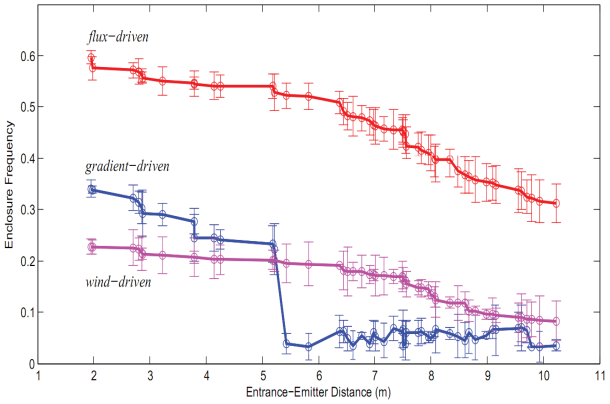

Fig. 8. Emitter enclosure results for seven robots, averaged over 50 plume configurations. The x axis is the distance between the initial starting location of the robotic swarm and the emitter, and the y axis is the fraction of total CPT time (900 simulation steps) spent by the swarm surrounding the emitter.

Enclosure Simulations

To evaluate the CPT performance of the modeled robotic swarm, we selected different flow conditions containing a dynamic, airborne plume spread over a 100 m^2 region. Flow parameters were identical for each environment, but the plumes differed because of the obstacles and the emitter locations (see Fig. 5). We compared gradient-driven, wind-driven, and flux-driven approaches on a suite of 50 simulated, realistic plume scenarios with different emitter locations. A total of 1500 CPT evaluation runs were performed in this experimental set (10 runs per emitter, CPT strategy). In each CPT run, the chemical was ejected for 100 simulation steps (about 100 seconds of real plume time) prior to lattice deployment. We then advanced the plume for 900 steps (corresponding to a realistic 15 minutes CPT run), and computed the percentage of time that the chemical source was surrounded by the seven-agent lattice, i.e., the enclosure frequency. This metric allows us to capture the stability and robustness characteristics of each CPT algorithm. Starting locations of the robots were limited in a 1 m^2 square area near the entrance door.

In this set of experiments, the maximum formation radius for flux-driven approach was set at one meter, to match the scale of plume features. Based on prior test results indicating that the performance of gradient- and wind-driven approach is more consistent with a fixed-radius formation, the VP force law for these two algorithms executed with the desired inter-vehicle spacing set at 0.5 meter.

The outcome of enclosure tests is plotted in Fig. 8. The amount of time the lattice spent encircling the emitter is an important evaluation criterion because it measures how precise and consistent a CPT algorithm is at determining the location of the plume's stationary source. To measure this criterion, we used a global observer (strictly during the evaluation stage), and computed the time fraction that the robotic lattice spent surrounding the chemical emitter.

From the plot, note that flux-driven (mean=0.447) significantly outperformed gradient-driven (mean=0.101) and wind-driven (mean=0.147). Since wind-driven always moves upwind in the plume, it often overshoots the emitter, and spends 80% of its CPT time in a cycle of first moving upstream in the plume and then casting after missing the emitter. Gradient-driven does somewhat better, but its performance falls off rapidly, caused by the obstacle-induced local density maxima. Due to the turbulence in the flow, and the resulting periodic chemical shedding effect, the lattice often fails to contain the source.

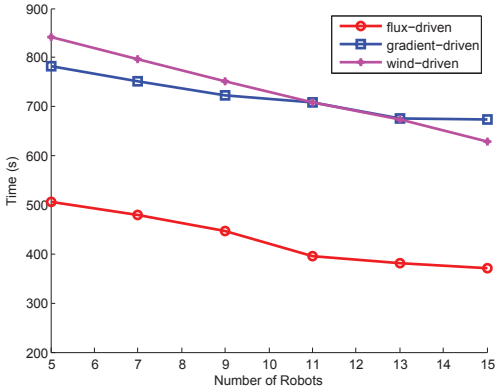

Fig. 9. Arrival time results for each CPT algorithm averaged over 50 emitter locations. Lower values indicate better performance.

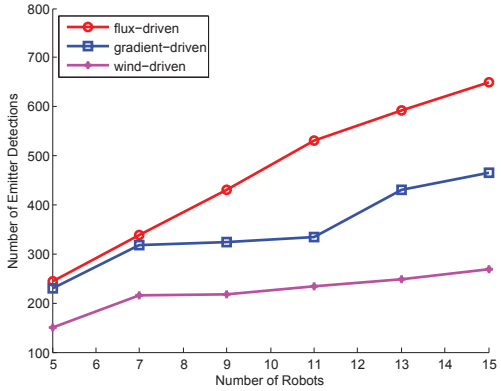

Fig. 10. Emitter detection by swarms of different size, averaged over 50 emitter locations. Larger values indicate higher performance.

Scalability Simulations

The set of experiments presented in this section focuses on the impact that increasing the swarm size has on CPT performance. The experimental methodology in this second investigation is consistent with that of the first study. Robotic swarms of varying sizes, controlled by the VP framework, navigated through a test suite of environments with 50 randomly created emitter locations. The CPT performance scores are reported as averages over the combination of each flow configuration, using swarm size as the independent variable.

Consistent with our previous simulations, we allow for 100 steps of initial chemical contamination before deploying the robots. The starting location of the swarm was set randomly to a limited 4 m^2 area near the entrance door. The number of vehicles in the swarm varied from 5 to 15 robots, with 2 robot increments (a total of 3000 CPT evaluation runs were performed for this study, 10 runs per emitter, swarm size). The evolution of each plume spanned 900 time steps, and for each CPT algorithm we recorded the time of the first sensor contact with the emitter by any robot in the swarm (the time of first detection metric), and the total number of emitter detections by the whole swarm during the entire CPT scenario (the localization frequency metric).

The amount of time each CPT algorithm spent searching for the emitter is plotted in Fig. 9. The count of successful source localizations for each swarm size is shown in Fig. 10. The first observation from the two plots is that only flux-driven approach performs well on both metrics; it combines the speed performance demonstrated by wind-driven, with the good emitter detection frequency of gradient-driven. Flux-driven is a robust, efficient, theory-based solution for a complex problem, that uses the available information about the underlying physical process to consistently improve the swarm's performance.

The intelligent utilization of data from the distributed sensor nodes is an emergent property of the swarm, arising from the lattice arrangement of the agents, which in turn is facilitated by the VP framework. By sharing the information about local flow conditions between neighboring vehicles in the group, each team member is able to construct a more accurate view of the surrounding plume. Furthermore, through the application of fluid mechanics, the set of vehicle waypoints selected by flux-driven is shown to be more effective in finding the emitter than the paths chosen by the more heuristic algorithms.

Figure 10 highlights another important finding: CPT is inherently a swarm application, because of the gain in performance achieved with an increase in the swarm size. A clue to the difference in localization performance between gradient-driven and wind-driven lies in the fact that wind-driven does not share plume observations amongst neighboring vehicles, but simply navigates upstream in the local airflow. Gradient-driven however, computes the local gradient of the chemical concentration, thus gaining more information about the behavior of the plume in the vicinity of each vehicle, and benefiting from the multiplicity of the sensor nodes.

Summary and Future Work

In this paper we presented a virtual-physics based control framework for swarm robotic chemical plume tracing and emitter localization problem. Simulation results show that the proposed control framework and flux-driven tracing strategy can effectively navigate the multi-robot system to the chemical emitter region. The virtual-physics based framework is highly flexible, endows the robot formation the properties of self-organization and self-repair. The mass-flux-driven plume tracing can inhibit the robots from adhering to plume "trap" and guide the robots forward to the real source region.

We showed that a challenging real-world problem, characterized by a complicated set of non-linear interactions, can in fact be solved in a fully distributed manner by using simple, inexpensive mobile sensor platforms. The effectiveness of VP framework comes from the firm foundation in Newtonian physics. Hence the robotic swarm is predictable autonomous, with an exceptionally low number of control parameters. Furthermore, by extending the physical model from vehicle formation control to sensor information management, it can be an effective search and rescue system to identify the location of a chemical source.

Our future work includes large scale advanced turbulence plume models and parameters optimization to test the performance of the presented methodology. On the other hand, we will validate the algorithm via transiting it to the real swarm robotic platform.

Acknowledgement

The work reported in this paper is supported by the National Natural Science Foundation of China (Grant No. 61175108) and the National High Technology Research and Development Program of China (Grant No. 2011AA040902).

REFERENCES

[1] W. Spears, D. Spears, J. Hamann, and R. Heil, "Distributed, physics-based control of swarms of vehicles," *Autonomous Robots*, vol. 17, no. 2, pp. 137–162, 2004.

[2] N. Vickers, "Mechanisms of animal navigation in odor plumes," *Biological Bulletin*, vol. 198, no. 2, pp. 203–212, 2000.

[3] X. Kang, W. Li, H. Xu, X. Feng, and Y. Li, "Validation of an odor source identification algorithm via an underwater vehicle,"

in *2012 Int. Conf. Intelligent System Design and Engineering Application*, pp. 740–743, IEEE, 2012.
[4] R. Russell, D. Thiel, R. Deveza, and A. Mackay-Sim, "A robotic system to locate hazardous chemical leaks," in *Proc. of the 1995 IEEE Int. Conf. Robotics and Automation*, vol. 1, pp. 556–561, 1995.
[5] H. Ishida, T. Nakamoto, and T. Moriizumi, "Remote sensing of gas/odor source location and concentration distribution using mobile system," *Sensors and Actuators B: Chemical*, vol. 49, no. 1-2, pp. 52–57, 1998.
[6] F. Grasso, T. Consi, D. Mountain, and J. Atema, "Locating odor sources in turbulence with a lobster inspired robot," *From Animals to Animats*, vol. 4, pp. 104–112, 1996.
[7] A. Lilienthal, A. Zell, M. Wandel, and U. Weimar, "Sensing odour sources in indoor environments without a constant airflow by a mobile robot," in *Proc. of the 2001 IEEE Int. Conf. Robotics and Automation*, vol. 4, pp. 4005–4010, 2001.
[8] A. Ramirez, A. Lopez, A. Rodríguez, A. de Albornoz, and E. De Pieri, "An infotaxis based odor navigation approach," in *2011 ISSNIP Biosignals and Biorobotics Conf.*, pp. 1–6, IEEE, 2011.
[9] A. Farah and T. Duckett, "Reactive localisation of an odour source by a learning mobile robot," in *Proc. of the 2nd Swedish Workshop on Autonomous Robotics*, pp. 29–38, 2002.
[10] J. Farrell, J. Murlis, X. Long, W. Li, and R. Cardé, "Filament-based atmospheric dispersion model to achieve short time-scale structure of odor plumes," *Environmental Fluid Mechanics*, vol. 2, no. 1, pp. 143–169, 2002.
[11] A. Hayes, A. Martinoli, and R. Goodman, "Swarm robotic odor localization," in *Proc. of the 2001 IEEE Int. Conf. Intelligent Robots and Systems*, vol. 2, pp. 1073–1078, 2001.
[12] Y. Zou, D. Luo, and W. Chen, "Swarm robotic odor source localization using ant colony algorithm," in *Proc. of the 2009 IEEE Int. Conf. Control and Automation*, pp. 792–796, 2009.
[13] Q. Meng, W. Yang, Y. Wang, and M. Zeng, "Multi-robot odor-plume tracing in indoor natural airflow environments using an improved aco algorithm," in *2010 IEEE Int. Conf. Robotics and Biomimetics*, pp. 110–115, IEEE, 2010.
[14] S. Hettiarachchi and W. Spears, "Physicomimetics for mobile robot obstacle avoidance," in *2012 13th ACIS Int. Conf. Software Engineering, Artificial Intelligence, Networking and Parallel & Distributed Computing*, pp. 444–450, IEEE, 2012.
[15] J. Crimaldi, M. Koehl, and J. Koseff, "Effects of the resolution and kinematics of olfactory appendages on the interception of chemical signals in a turbulent odor plume," *Environmental Fluid Mechanics*, vol. 2, no. 1, pp. 35–64, 2002.
[16] J. Hurtado, R. Robinett, C. Dohrmann, and S. Goldsmith, "Distributed sensing and cooperating control for swarms of robotic vehicles," in *Proc. of the 1998 IASTED Conf. Control and Applications*, pp. 175–178, 1998.
[17] G. Sandini, G. Lucarini, and M. Varoli, "Gradient driven self-organizing systems," in *Proc. of the 1993 IEEE Int. Conf. Intelligent Robots and Systems*, vol. 1, pp. 429–432, 1993.
[18] S. Kazadi, "Extension of plume tracking behavior to robot swarms," in *Proc. of the 2003 World Multi Conf. Systemics, Cybernetics and Informatics*, 2003.
[19] M. Wandel, A. Lilienthal, T. Duckett, U. Weimar, and A. Zell, "Gas distribution in unventilated indoor environments inspected by a mobile robot," in *Proc. of the 2003 IEEE Int. Conf. Advanced Robotics*, pp. 507–512, 2003.
[20] R. Russell and A. Purnamadjaja, "Odor and airflow: Complementary senses for a humanoid robot," in *Proc. of the 2002 IEEE Int. Conf. Robotics and Automation*, vol. 2, pp. 1842–1847, 2002.
[21] H. Ishida, T. Nakamoto, T. Moriizumi, T. Kikas, and J. Janata, "Plume-tracking robots: A new application of chemical sensors," *Biological Bulletin*, vol. 200, no. 2, pp. 222–226, 2001.
[22] J. Farrell, S. Pang, and W. Li, "Plume mapping via hidden markov methods," *IEEE Trans. on Systems, Man, and Cybernetics, Part B: Cybernetics*, vol. 33, no. 6, pp. 850–863, 2003.
[23] S. Pang and J. Farrell, "Chemical plume source localization," *IEEE Trans. on Systems, Man, and Cybernetics, Part B: Cybernetics*, vol. 36, no. 5, pp. 1068–1080, 2006.
[24] A. Loutfi, S. Coradeschi, and J. Gonzalez, "Gas distribution mapping of multiple odour sources using a mobile robot," *Robotica*, vol. 27, no. 2, pp. 311–319, 2009.
[25] A. Lilienthal and T. Duckett, "Building gas concentration gridmaps with a mobile robot," *Robotics and Autonomous Systems*, vol. 48, no. 1, pp. 3–16, 2004.
[26] A. Hayes, A. Martinoli, and R. Goodman, "Distributed odor source localization," *IEEE Sensors Journal*, vol. 2, no. 3, pp. 260–271, 2002.
[27] R. Russell, "Laying and sensing odor markings as a strategy for assisting mobile robot navigation tasks," *IEEE Robotics and Automation Magazine*, vol. 2, no. 3, pp. 3–9, 1995.
[28] D. Zarzhitsky, D. Spears, and W. Spears, "Distributed robotics approach to chemical plume tracing," in *Proc. of the 2005 IEEE Int. Conf. Intelligent Robots and Systems*, pp. 4034–4039, 2005.
[29] X. Cui, T. Hardin, R. Ragade, and A. Elmaghraby, "A swarm-based fuzzy logic control mobile sensor network for hazardous contaminants localization," in *Proc. of the 2004 IEEE Int. Conf. Mobile Ad-hoc and Sensor Systems*, pp. 194–203, 2004.
[30] J. T. Feddema, R. D. Robinett, and R. H. Byrne, "An optimization approach to distributed controls of multiple robot vehicles," in *Workshop on Control and Cooperation of Intelligent Miniature Robots, IEEE Int. Conf. Intelligent Robots and Systems*, 2003.
[31] M. Polycarpou, Y. Yang, and K. Passino, "Cooperative control of distributed multi-agent systems," *IEEE Control Systems Magazine*, 2001.
[32] W. Spears and D. Gordon, "Using artificial physics to control agents," in *Proc. of the 1999 IEEE Int. Conf. Information Intelligence and Systems*, pp. 281–288, 1999.
[33] O. Khatib, "Real-time obstacle avoidance for manipulators and mobile robots," *International Journal of Robotics Research*, vol. 5, no. 1, p. 90, 1986.
[34] C. Belta and V. Kumar, "Trajectory design for formations of robots by kinetic energy shaping," in *Proc. of the 2002 IEEE Int. Conf. Robotics and Automation*, vol. 3, pp. 2593–2598, 2002.
[35] J. Fax and R. Murray, "Information flow and cooperative control of vehicle formations," *IEEE Trans. on Automatic Control*, vol. 49, no. 9, pp. 1465–1476, 2004.
[36] D. EDWARDS, T. BEAN, D. ODELL, and M. ANDERSON, "A leader-follower algorithm for multiple auv formations," in *Proc. of the IEEE/OES Autonomous Underwater Vehicles Conf.*, pp. 40–46, 2004.
[37] C. Frey, D. Zarzhitsky, W. Spears, D. Spears, C. Karlsson, B. Ramos, J. Hamann, and E. Widder, "A physicomimetics control framework for swarms of autonomous surface vehicles," in *Proc. of the OCEANS 2008*, pp. 1–6, 2008.
[38] A. Lilienthal and T. Duckett, "A stereo electronic nose for a mobile inspection robot," in *Proc. of the 2003 Int. Workshop Robotic Sensing*, 2003.

***Authors**: Ph.D. student Yuhua ZOU, School of Automation Science and Electrical Engineering, Beihang University, 37 Xueyuan Road, Haidian District, Beijing 100191, P.R. China, email: chenyusiyuan@126.com; Prof. Weihai CHEN, School of Automation Science and Electrical Engineering, Beihang University, 37 Xueyuan Road, Haidian District, Beijing 100191, P.R. China, email: whchenbuaa@126.com; Prof. Dehan LUO, School of Information Engineering, Guangdong University of Technology, 100 Waihuan Xi Road, Guangzhou Higher Education Mega Center, Guangzhou 510006, P.R. China, email: dehanluo@gdut.edu.cn*